

Heterogeneous structure of a magnetohydrodynamic mixer made by the LTCC process using a photoimageable slurry

Jaekyung Choi^{a,b}, Young Joon Yoon^{a,*}, Youn-Suk Choi^c, Hyo Tae Kim^a, Jihoon Kim^a, Jong-Heun Lee^b and Jong-hee Kim^a

^aNano-IT Convergence Center, Korea Institute of Ceramic Engineering & Technology, 233-5 Gasan-dong, Gueancheon-gu, Seoul 153-801, Korea

^bDept. of Materials Science and Engineering, Korea University, Anam-dong, Seongbuk-gu, Seoul 136-701, Korea

^cKyungwon EnC, Rm 704 Woolim Lions Valley 1, 311-3 Sangdaewon-dong, Jungwon-gu, Sunghnam-si, Gyeonggi-do 462-806, Korea

A novel microfabrication process for the creation of a magnetohydrodynamic (MHD) mixer is presented using a photoimageable low temperature co-fired ceramic (LTCC). A monolithic structure was formed by UV photolithographic patterning and screen printing. The structure consists of a microfluidic channel and silver electrodes on a LTCC layer. The fluids in the microfluidic channel were controlled by a Lorentz force. A maximum mixing efficiency of 85.4% was achieved with AC peak-to-peak voltages of 8 V at 1 Hz. A photolithographic technique for patterning the microfluidic channel in the LTCC process is promising in order to realize a complex heterogeneous structure and it serves as an enabling tool in extending the applicability of ceramic-based microfluidic devices.

Key words: Magnetohydrodynamic, Microfluidic, Mixer, LTCC, Photolithography.

Introduction

Lab-on-a-chip (LoC) has been an emerging technology for biomedical applications including point-of-care testing diagnosis and ubiquitous healthcare systems [1-3]. However, there are still many issues involved in making a more complete LoC system. LoC technology requires the incorporation of various functional components, such as a micro-chamber, microchannel, micropump, microvalve, micro-mixer, sensor, and power source, on a single microfluidic platform [2-4]. Although it is possible to integrate various components with silicon-based MEMS fabrication technology, this cannot be used as a final solution due to its high cost. Low-cost polymer-based microfluidic devices have been studied widely during the last decade. However, difficulties in building up a heterojunction and in the integration of components must be solved in order to extend their applications. Recently, low temperature co-fired ceramic (LTCC) materials, which have been used for multi-chip ceramic modules, are being applied to the fabrication of simple microfluidic structures [5-10]. LTCC was suggested as a potential alternative for the production of two- or three-dimensional microfluidic modules; it has the unique advantage of efficient integration capability on account of its hybrid nature.

This paper presents a LTCC-based fabrication technology

to make a heterogeneous microfluidic structure of a magnetohydrodynamic (MHD) mixer. A MHD-based microfluidic system can be applied to micro-pumps, stirrers, networks, and analytical devices [9-13]. A metal electrode and insulating ceramic channel in our MHD mixer were made by screen printing and photolithographic patterning, respectively. The MHD mixer uses a Lorentz force to achieve mixing. The force for manipulation of conducting fluids depends on the magnitude and direction of the electric and magnetic fields. The mixing performance of the fabricated device was evaluated by tracing the fluorescence intensity, which is varied according to the electrical condition under a given magnetic field.

Experiment

Device fabrication

To fabricate the MHD mixer, LTCC technology combined with thick film photolithography was employed. The basic photosensitive slurry was composed of ceramic powders, photo-initiators, monomers, plasticizers, sensitizers and a solvent. The main ceramic material was Ca-modified amorphous cordierite ($(\text{Mg}, \text{Ca})_2\text{Al}_4\text{Si}_5\text{O}_{18}$) with an average particle size of 2 μm . The solid loading in the slurry was kept to 48 wt% for the tape casting process. Fig. 1 describes the fabrication process of the MHD mixer based on the LTCC process with photolithographic patterning. A conventional LTCC sheet for a base plate and a photoimageable LTCC sheet were produced for a microfluidic channel with a 50 μm thickness, using the tape casting process. First, a rigid base plate was prepared through lamination of twenty

*Corresponding author:
Tel : +82-2-3282-7854
Fax: +82-2-3282-7838
E-mail: yjyoon@kicet.re.kr

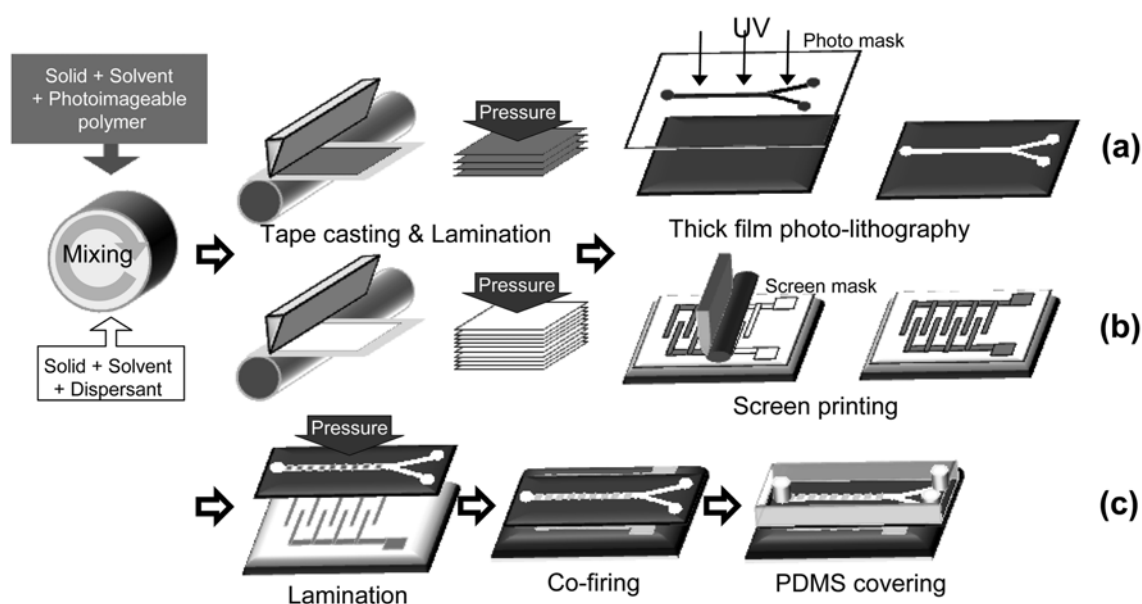


Fig. 1. Schematic showing the fabrication process for the MHD mixer using LTCC and thick film photolithography. (a) microfluidic channel formed by UV photolithography, (b) metal electrode patterned by screen printing, and (c) a monolithic structure formed by lamination and co-firing.

LTCC sheets without photosensitive components. Then, the Ag electrode was patterned using the screen printing method with a 400-mesh screen. To obtain a microfluidic channel, five sheets of laminated photoimageable LTCC layer were exposed to 365 nm ultra-violet (UV) light using a photo mask. After UV exposure for 1 minute, hardening of the photosensitive slurry was initiated by the polymerization of monomers. The microfluidic channel was formed following a developing process. After careful alignment and lamination of the photoimageable layers, which included the microfluidic channel on a base plate with Ag electrode patterns, a monolithic structure was obtained. A green ceramic body was co-fired at 800 °C for 1 hour in air. The body then underwent air plasma treatment (26.7 Pa, 200 W) using an expanded plasma cleaner (Harrick Science, NY) for 30 s [14]. Finally, a transparent PDMS cover was irreversibly bonded to the sintered ceramic body.

Microfluidic experiment

For optical quantification of the mixing efficiency, two types of fluids, a 2 mM fluorescein (F2456; Sigma-Aldrich, St. Louis, MO) solution dissolved in a 0.24 M Na₂CO₃ aqueous solution and de-ionized water, were prepared. Inlet and outlet ports with 1 mm diameter holes were punched into the PDMS cover using a sharpened needle. Tygon tubes (S-54-HL, Harvard Apparatus, Holliston, MA) were inserted into the holes to make a fluidic connection with a syringe pump. Working solutions were injected into the device by a micropump (Pump 11 pico plus; Harvard Apparatus, Holliston, MA) at a 72 $\mu\text{l}\text{minute}^{-1}$ flow speed. To generate the Lorenz force, an AC voltage was applied with a function generator (AGF3011; Tektronix, Beaverton, OR). To maintain a uniform magnetic field, a permanent

magnet of 0.5 T magnetic flux density, about 25 times larger in size than the microfluidic channel, was positioned under the MHD device. The mixing efficiency of the device was quantified by an optical determination of the fluorescence intensity of the working fluids during the mixing process. The diffused fluorescence images were captured by a SteREO Discovery V12 (Zeiss, Oberkochen, Germany) microscope with a MacroFire charge-coupled device (CCD) camera (Optronics, Goleta, CA). The quantification process is described in more detail in the following section.

Results and Discussion

Fig. 2(a) describes the schematic and working mechanism of the MHD mixer. The microfluidic channel fabricated by photolithographic patterning was 2.0 mm wide and 20.7 mm long. Ag electrode patterns had a width of 500 μm and a period of 1.5 mm. In this study, an AC electricity source of 2-8 V_{pp} (1 Hz to 1 kHz) was used to prevent bubble generation. This would have occurred under a DC source due to rigorous electrolysis of the Na₂CO₃ aqueous solution, which has a conductivity of 27 mS/cm [15]. Therefore, the direction of the Lorenz force, which was perpendicular to both the electric and magnetic fields, was altered periodically in our experimental setup.

Optical images of the MHD mixer, after fabrication of the green body by stacking electrodes and the microfluidic channel on a base plate, are shown in Fig. 2(b). The height of the microfluidic channel was approximately 200 μm after lamination of five photoimageable sheets. It was clearly confirmed that a monolithic structure, made up of the microfluidic channel and the Ag electrode on a base plate, was formed successfully by photolithographic patterning

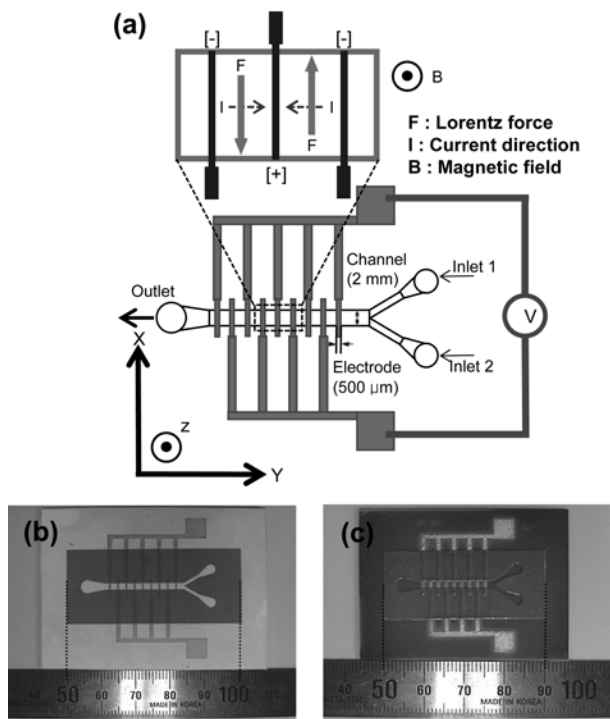


Fig. 2. (a) Schematic of the MHD mixer illustrating how the Lorentz force is formed by the electric and magnetic fields, (b) Optical image of the MHD mixer after lamination, and (c) Optical image of the MHD mixer after co-firing at 800 $^{\circ}\text{C}$.

and screen printing. In the LTCC process, shrinkage of the ceramic body, including embedded electronic circuits, was inevitable after the co-firing process. It was observed in our device that the ratio of shrinkage in the x-y and z directions was approximately 20% and 15%, respectively. However, significant micro-cracking or delamination of the whole surface and interface were not observed after the sintering process at 800 $^{\circ}\text{C}$, as shown in Fig. 2(c).

Fig. 3 shows fluorescent images of the hydrodynamic disturbance of fluids under AC peak-to-peak voltages between 2 and 8 V at 1 Hz. As shown in Fig. 3(a), the planar interface between the two fluids was still maintained under 2 V_{pp} . At 5 V_{pp} , vibration of the fluid interface was initiated due to the Lorentz force. This vibration was maximized at 8 V_{pp} . In Fig. 3(b) and (c), it can be clearly observed that the direction of the flow was manipulated periodically with the changes of polarity of the electrodes at 8 V_{pp} . Therefore, it was deduced that considerable mixing of fluids could be accomplished due to the increase of the interfacial surface, as compared to the condition of Fig. 3(a).

Fig. 4(a) shows the fluorescence intensity profile along the channel width near the outlet region with increasing AC peak voltage. It was impossible to increase the AC voltage up to 10 V_{pp} due to the formation of too many bubbles. First, the fluorescent intensity was converted into a gray scale for numerical analysis using imageJ software (<http://rsb.info.nih.gov/ij/>) to calculate the mixing efficiency. It was normalized with respect to working solutions (taking 2 mM fluorescein solution dissolved in 0.24 M Na_2CO_3

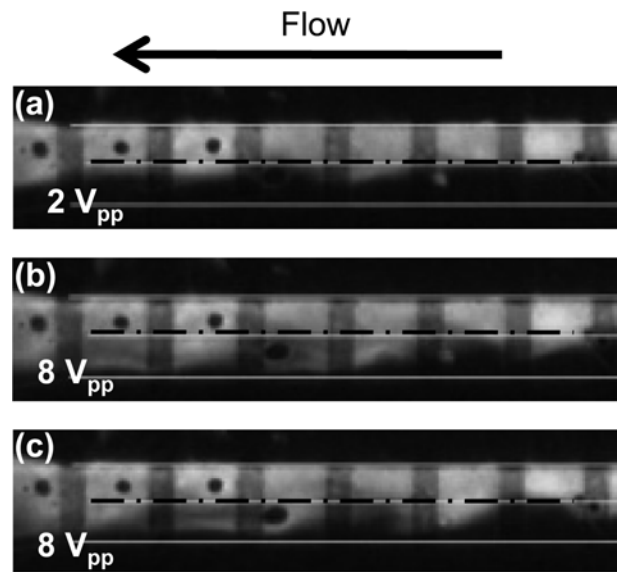


Fig. 3. Fluorescent micrographs showing oscillation of fluids in the MHD mixer with variation of the AC peak-to-peak voltages at 1 Hz (a) 2 V_{pp} . Fig. 3 (b) and (c) were obtained using 8 V_{pp} at different phases.

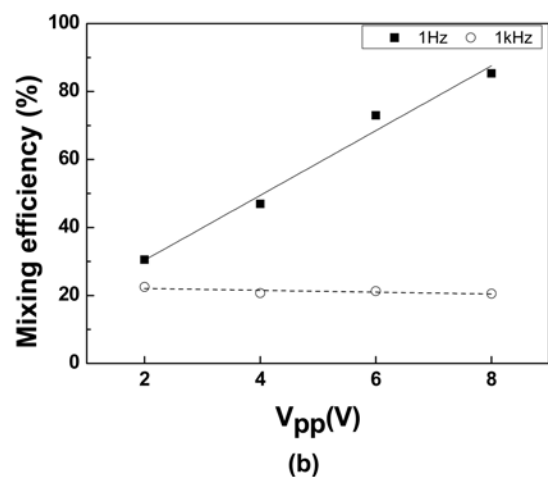
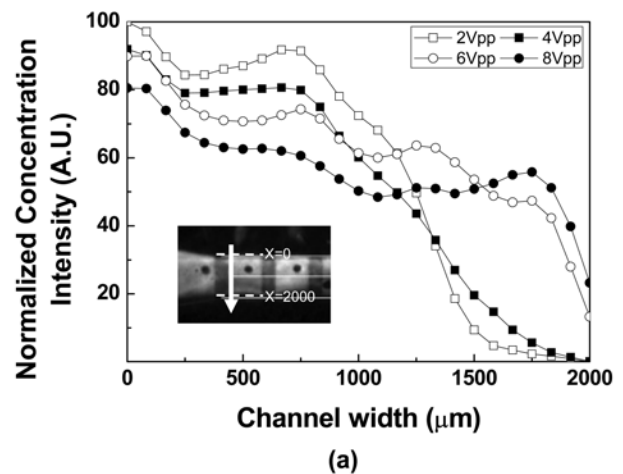


Fig. 4. (a) Fluorescence concentration profile across the channel (2,000 μm) as a function of the applied AC voltage, (b) Calculated mixing efficiency versus the applied AC voltage with a variation of the frequency.

aqueous solution as 100% and de-ionized water as 0%, respectively) and was expressed in terms of the concentration. The mixing efficiency (η) across the channel width (w) is defined as:

$$\eta = \left(1 - \frac{\int_0^w |c - c_\infty| dw}{\int_0^w |c_0 - c_\infty| dw} \right) \times 100 \quad (1)$$

where c is the fluorescence intensity across the channel width at the outlet, c_∞ is the intensity in the case of perfect mixing ($= 0.5$), and c_0 is the initial intensity before any mixing [16-17]. It was revealed that the mixing efficiency increased linearly with the increase of the AC voltage amplitude, and a maximum mixing efficiency of 85.4% could be achieved with $8 V_{pp}$ at 1 Hz. Considerable mixing was caused by an increase of the interfacial boundary due to the disturbance of fluids controlled by the Lorentz force as mentioned earlier. At a higher frequency of 1 kHz, however, a negligible diffusive mixing efficiency of about 20% was obtained. We speculate that the incomplete mixing at high frequency was caused by the inertial force of the working fluids. The active mixing efficiency is governed by the fluidic force of the MHD. However, even under a given active convection, a certain time interval is required before the polarity of the applied voltage changes. This voltage change forms a wavy interface between the two streams due to the inertia of the moving entities. It seemed that a frequency of 1 kHz was too high to fully transfer the forced convective momentum into the fluids in our system.

This paper describes a heterogeneous microfluidic structure of a MHD mixer, which was operated with an experimental set-up consisting of an AC source and a permanent magnet. This simple configuration resulted in considerable oscillation of the fluid for efficient mixing. The optimum condition without the formation of bubbles could be improved by tuning the design of the microfluidic structure.

Conclusion

In this study, the microfabrication of a ceramic-based MHD mixer using the LTCC process combined with thick film photolithography was presented. A photoimageable slurry was developed by mixing amorphous cordierite and photosensitive polymers. It showed good performance in making a microfluidic channel by UV photolithography. A combination between photolithography and LTCC processes, in comparison to conventional a micromachining process using computerized numerical control (CNC) or

laser milling, provide a simple approach to fabricate complex channel and cavity structures, which can also be applicable to various microfluidic or electronic devices. It was confirmed that the ceramic-based MHD mixer worked well under a variation of AC voltage, showing a sufficient oscillation of fluids for mixing. We believe that the magnetohydrodynamic phenomenon enables a ceramic-based microfluidic device to extend its applications, including pumping, stirring or mixing of fluids.

Acknowledgement

This work was supported from the R&D program by Korea Institute of Ceramic Engineering and Technology.

References

1. H. Andersson and A.V.D. Berg, *Sensors and Actuators B* 92 (2003) 315-325.
2. P. Abgrall and A.-M. Gue, *J. Micromech. Microeng.* 17 (2007) R15-R49.
3. C.H. Ahn, J.-W. Choi, G. Beaucage, J.H. Nevin and J.-B. Lee, A. Puntambekar and J.Y. Lee, *Proceedings of the IEEE* 92 (2004) 154-173.
4. J.-C. Yoo, M.-C. Moon, Y.J. Choi, C.J. Kang and Y.-S. Kim, *Microelectronic Engineering* 83 (2006) 1684-1687.
5. L.J. Golonka, *Bulletin of Polish Academy of Sciences Technical Sciences* 54 (2006) 221-231.
6. I. Wyzkiewicz, N. Lewandowska, M. Chudy, Z. Brzozka, Z. Magonski, B. Dziurdzia, M. Jakubowska and A. Dybko, *Microsyst. Technol.* 13 (2007) 657-661.
7. L.J. Golonka, H. Roguszczyk, T. Zawada, J. Radojewski, I. Grabowska, M. Chudy, A. Dybko, Z. Brzozka, D. Stadnik, *Sensors and Actuators B* 111-112 (2005) 396-402.
8. Y.J. Yoon, J. Choi, J.-W. Lim, H.T. Kim, J. Kim, Y.-S. Choi, J.-H. Lee and J.-H. Kim, *Advanced Materials Research* 74 (2009) 303-306.
9. H.H. Bau, J. Zhong and M. Yi, *Sensors and Actuators B* 79 (2001) 207-215.
10. J. Zhong, M. Yi and H.H. Bau, *Sensors and Actuators A* 96 (2002) 59-66.
11. A.V. Lemoff and A.P. Lee, *Sensors and Actuators B* 63 (2000) 178-185.
12. S. Qian and H.H. Bau, *Mechanics Research Communications* 36 (2009) 10-21.
13. N.-T. Nguyen and Z. Wu, *J. Micromech. Microeng.* 15 (2005) R1-R16.
14. C.S. Lee, H.W. Shim, J.H. Lee and J.H. Jung, *Polymer Science and Technology*, 17[2] (2006) 191-206.
15. V. Studer, A. Pe'pin, Y. Chen and A. Ajdari, *Microelectronic Engineering* 61-62 (2002) 915-920.
16. N.L. Jeon, S.K.W. Dertinger, D.T. Chiu, I.S. Choi, A.D. Stroock and G.M. Whitesides, *Langmuir* 16 (2000) 8311-8316.
17. V. Hessel, H. Lowe and F. Schonfeld, *Chemical Engineering Science* 60 (2005) 2479-2501.